



Cite this: *Dalton Trans.*, 2016, **45**, 13415

Mono- and multimeric ferrocene congeners of quinoline-based polyamines as potential antiparasitics†

Tameryn Stringer,^a Carmen De Kock,^b Hajira Guzgay,^c John Okombo,^{a,b} Jenny Liu,^d Sierra Kanetake,^d Jihwan Kim,^d Christina Tam,^e Luisa W. Cheng,^e Peter J. Smith,^b Denver T. Hendricks,^c Kirkwood M. Land,^d Timothy J. Egan^a and Gregory S. Smith^{*a}

A series of mono- and multimeric polyamine-containing ferrocenyl complexes containing a quinoline motif were prepared. The complexes were characterised by standard techniques. The molecular structure of the monomeric salicylaldimine derivative was elucidated using single crystal X-ray diffraction and was consistent with the proposed structure. The antiplasmodial activity of the compounds were evaluated *in vitro* against both the NF54 (chloroquine-sensitive) and K1 (chloroquine-resistant) strains of *Plasmodium falciparum*. The polyamine derivatives exhibit good resistance index values suggesting that these systems are beneficial in overcoming the resistance experienced by chloroquine. Mechanistic studies suggest that haemozoin formation may be the target of these quinoline complexes in the parasite. Some of the complexes exhibit moderate to high cytotoxicity against WHCO1 oesophageal cancer cells *in vitro*. The monomeric ferrocenyl-amine complexes exhibit potent activity against this particular cell line. The complexes were also screened against the G3 strain of *Trichomonas vaginalis* and the salicylaldimine complexes demonstrated promising activity at the tested concentration. All of these compounds show no inhibitory effect on several common normal flora bacteria, indicative of their selectivity for eukaryotic pathogens and cancer.

Received 7th July 2016,
Accepted 26th July 2016
DOI: 10.1039/c6dt02685k

www.rsc.org/dalton

Introduction

Malaria is a parasitic disease that exists in both tropical and subtropical regions of various continents including Africa and Asia. The World Health Organisation (WHO) reported 198 million cases of malaria globally in 2013, of which 584 000 deaths were documented.¹ Antimalarial treatments are available to combat the disease, but drug resistance is an ongoing problem as *Plasmodium falciparum* rapidly develops resistance. Since 2000, artemisinin therapy has been the main treatment of the disease. Unfortunately, some reports of artemisinin resistance has surfaced in recent years.² To overcome this, suit-

able alternatives are imperative. Recently, attention has been turned to the use of metal-based compounds as potential antimalarials.^{3–5} Ferrocene, in particular, has been of interest due to its versatile nature. A promising lead, ferroquine (FQ) (Fig. 1), has exhibited the ability to overcome resistance experienced by its parent non-metal containing congener, chloro-

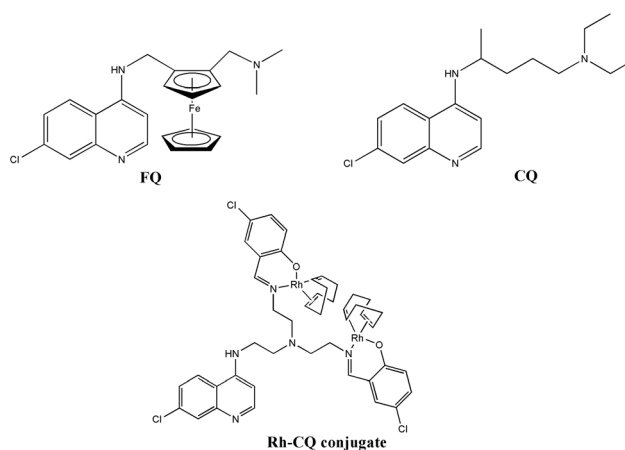


Fig. 1 Structures of ferroquine, chloroquine and a Rh-CQ conjugate¹⁰ that display promising antiplasmodial activity.

^aDepartment of Chemistry, University of Cape Town, Rondebosch 7701, South Africa. E-mail: Gregory.Smith@uct.ac.za

^bDivision of Pharmacology, Department of Medicine, University of Cape Town Medical School, Observatory 7925, South Africa

^cDivision of Medical Biochemistry, University of Cape Town, Rondebosch 7701, South Africa

^dDepartment of Biological Sciences, University of the Pacific, Stockton, CA 95211, USA

^eFoodborne Toxin Detection and Prevention Unit, Agricultural Research Service, United States Department of Agriculture, Albany, CA 94710, USA

† Electronic supplementary information (ESI) available. CCDC 1487428. For ESI and crystallographic data in CIF or other electronic format see DOI: 10.1039/c6dt02685k



quine (CQ) (Fig. 1). This compound is extremely active against various strains of *P. falciparum* *in vitro* as well as *in vivo* and has completed Phase IIB clinical trials.⁶ The success of FQ has prompted research towards many ferrocene-based quinoline analogues as potential antimalarials as these complexes are generally quite stable and easily prepared. Despite structural similarities, the activity of these compounds only weakly compare to that of FQ.^{3–5} This complex is believed to work by the same mechanism of action as chloroquine because it inhibits formation of haemozoin, a detoxification product of ferriprotoporphyrin(IX), that forms as a result of haemoglobin degradation. The build-up of the toxic porphyrin ultimately leads to parasite death. FQ is also thought to promote oxidative stress, due to its redox activity.⁷ It is able to generate reactive oxygen species (ROS) *via* a Fenton-like reaction, which results in irreversible damage towards the parasite.⁷ FQ also accumulates in the parasitic food vacuole to a greater extent than chloroquine which further increases its effectiveness. The lipophilicity, basicity and folded conformation of ferroquine allows for better transport through membranes and allows for better accumulation inside of the digestive vacuole of the parasite.⁷ In many cases, quinoline-containing ferrocenyl complexes have exhibited promising activity which is usually attributed to the presence of the quinoline moiety. Some non-quinoline based ferrocenes have also exhibited promising activities, including those that possess a thiosemicarbazone moiety.^{8,9} This particular moiety has been known to impart a range of biological properties. Multinuclear ferrocenyl complexes based on a polyamine scaffold have also been evaluated and display promising activity but do not compare in activity to many quinoline-based complexes. More recently, it has been shown that rhodium-based quinolines conjugated to a polyamine scaffold (Fig. 1) display comparable behaviour in both CQ-sensitive (CQS) and CQ-resistant (CQR) strains of *P. falciparum*.¹⁰ This showed that incorporation of the polyamine back-bone as well as increased metal nuclearity aids in overcoming the cross-resistance experienced by mononuclear analogues as well as CQ. The chloride-substituted complexes of these compounds have also shown activity against *Trichomonas vaginalis* – the protozoan causative agent of the sexually transmitted trichomoniasis prevalent in industrialised countries.^{10,11} The WHO has estimated that 160 million cases of this infection occurs annually worldwide.¹² This pathogen is usually treated with drugs such as metronidazole and tinidazole, however, drug resistance is currently on the rise. Based on the promising activity of some polyamine-derived quinolines as well as the success of ferroquine, this study aimed to prepare mono- and multimeric ferrocenyl-based quinolines based on polyamine scaffolds as potential antiparasitic agents. Ferrocene was incorporated to improve the antiparasitic activity; the polyamines were incorporated in order to maintain activity in resistant strains compared to sensitive strains. The quinoline moiety was incorporated to maintain antiplasmodial activity and to act as an inhibitor of haemozoin formation. Screening the entire library on normal flora and select pathogenic bacteria shows the specificity of

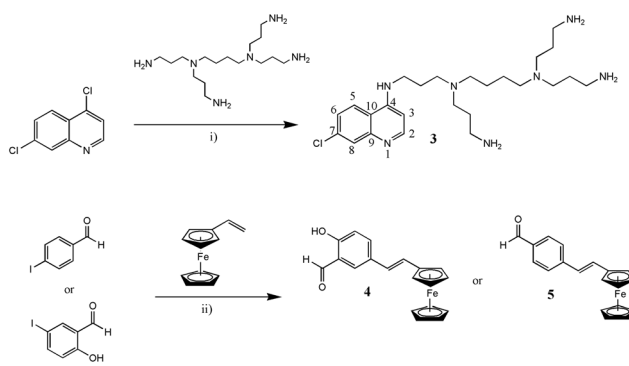
these compounds for eukaryotic cells, including protozoan parasites and cancer.

Results and discussion

Synthesis and characterisation

The Schiff base ferrocenyl complexes were prepared by the reaction of the respective mono-functionalised quinoline amines (1–3) with either 5-((*E*)-2-ferrocenylvinyl)-2-hydroxybenzaldehyde (4), 4-((*E*)-2-ferrocenylvinyl)benzaldehyde (5) or ferrocenecarboxaldehyde. *N*-(7-chloroquinolin-4-yl)-propane-1,3-diamine (1)¹³ and *N*-(7-chloroquinolin-4-yl)-tris(2-aminoethyl)amine (2)¹⁴ were prepared according to literature methods. Mono-functionalisation of DAB-Am-4 was achieved by a nucleophilic substitution reaction of 4,7-dichloroquinoline and excess generation 1 dendrimer giving rise to *N*-(7-chloroquinolin-4-yl)-tetrakis(3-aminopropyl)-1,4-butanediamine (3) (Scheme 1). Compound 3 exhibits good solubility in solvents such as MeOH, EtOH and DMSO. Mono-functionalisation of the polyamines were employed in order to conjugate ferrocene as part of these systems as well. The ferrocenyl moieties were incorporated as part of these scaffolds *via* ferrocenyl aldehydes 4 and 5. These were prepared by means of a Heck cross-coupling reaction of vinylferrocene and either 5-iodosalicylaldehyde or 4-iodobenzaldehyde (Scheme 1). Aldehyde 5 was prepared following a known literature methodology and its integrity was confirmed by ¹H NMR spectroscopy (ESI[†]).^{15,16}

In the ¹H NMR spectrum of 3, the integration is consistent with the mono-functionalised product, with distinctive signals observed for both the quinoline and the polyamine moieties. An absorption band at 1609 cm⁻¹ was observed in the infrared spectrum of 3, which is attributed to the C=N bond, confirming the presence of the quinoline moiety. The ESI mass spectrum also confirmed the integrity of 3 due to the appearance of a peak at *m/z* 520.3339 corresponding to [M + CH₃CN + H]⁺. The ¹H NMR spectra of 4 and 5 exhibited two doublets for the protons of the alkenyl groups, respectively. Coupling constants of approximately 16 Hz were observed which is consistent with similar coupled products with *trans* geometry.^{15,16} Signals for

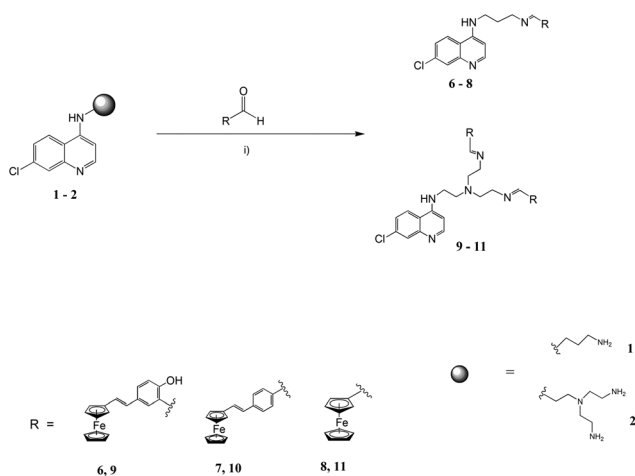


Scheme 1 Synthesis of quinoline 3 and ferrocenyl aldehydes 4 and 5 (i) Neat, 18 h, 90 °C; (ii) tri(*p*-tolyl)phosphine, Pd(OAc)₂, Et₃N, CH₃CN, 24 h, 90 °C.

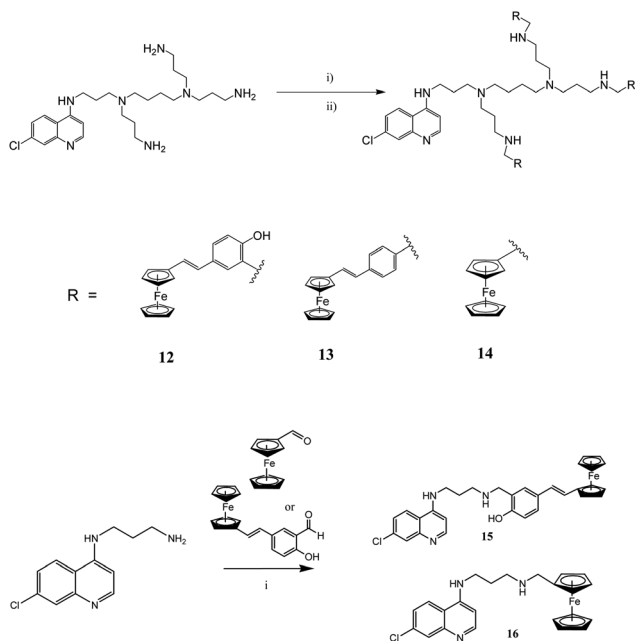


the protons of the aldehyde moieties were observed at 9.92 and 9.97 ppm for **4** and **5**, respectively.

Upon successful synthesis of the desired precursors, Schiff base condensation of the aldehydes and the various amines were carried out (Scheme 2). Imine complexes **6–11** were isolated as red or orange amorphous solids in various yields (21–85%). Due to some difficulties experienced in the purification of the DAB-derived imine compounds, the preparation of the amines (**12–14**) was carried out *via* one-pot reductive amination reactions (Scheme 3). Compounds **12–14** were afforded by addition of NaBH₄ to the intermediate imines, to



Scheme 2 Synthesis of Schiff base ferrocenyl quinolines **6–11** (i) DCM : MeOH (1 : 1) 24 h, rt (**6, 7, 9, 10**); Et₂O, 16 h, rt (**8**); EtOH, 16 h, rt (**11**).



Scheme 3 Synthesis of ferrocenyl quinolines **12–16** (i) DCM : MeOH (1 : 1), 24 h, rt; NaBH₄, DCM : MeOH, 6 h, rt.

afford the desired complexes as brown or orange solids in various yields (41–79%). Reduced versions of **6** and **8** were also synthesised (Scheme 3) in order to establish the effect of the incorporation of an amine (**15** and **16**) instead of an imine motif. Compound **15** was prepared similarly to compounds **12–14**. Compound **16** was prepared using literature methods and its integrity confirmed by ¹H and ¹³C{¹H} NMR spectroscopy (ESI⁺).^{17,18}

In the ¹H NMR spectra of compounds **6–11**, singlets for the imine moiety were observed in the region of 8.10 and 8.40 ppm. The protons of the unsubstituted Cp ring of the ferrocenyl entity was confirmed by the appearance of a singlet in the spectra of **6–11** between 4.13 and 4.31 ppm. Signals for the protons of the quinoline moiety were also observed in the expected region. For compounds **12–16** all the expected signals were accounted for. No signals for imine moieties were observed in the spectra of **12–16** and thus confirmed successful reductive amination. The NH protons are considered to be exchangeable and are sometimes not observed. For example, in the ¹H NMR spectrum of **16**, a broad signal at ~1.8 ppm is observed for water (slightly downfield from the usual shift of 1.56 ppm in CDCl₃) which may insinuate an interaction of the compound and the solvent *via* hydrogen bonding through the amino group, which may be a reason for this signal not being observed in the spectrum. This could apply to the complexes **12–14** as well. Absorption bands for the two C=N bonds are observed in most cases in the region of 1630 and 1610 cm⁻¹, while bands for the C=C moiety of **6, 7, 9** and **10** were observed in the region between 1580 and 1600 cm⁻¹ in the infrared spectra. The C=N stretching vibrations for **12–14** were observed between 1607 and 1611 cm⁻¹. The complexes were further characterised by high resolution ESI mass spectrometry and the data was consistent with the proposed structures.

Crystallographic data

The molecular structure of compound **6** (Fig. 2) was elucidated and selected bond lengths and angles are summarised in

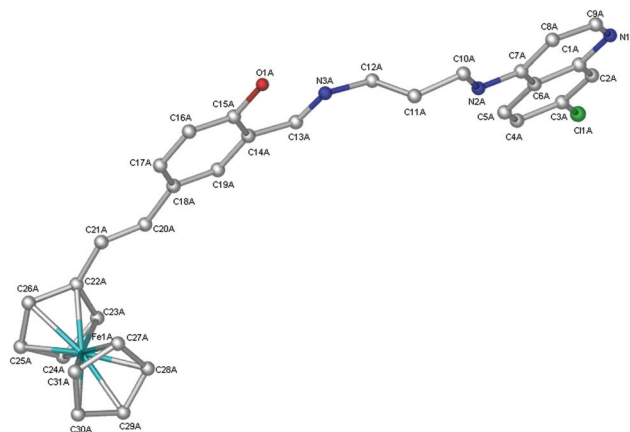


Fig. 2 Molecular structure of complex **6A**. Hydrogen atoms are omitted for clarity.



Table 1 Selected bond distances (Å) and angles (°) for complex **6A**

Entity	Bond distance (Å)/angle (°)
N3A–C13A	1.274(5)
C20A–C21A	1.343(6)
Cl1A–C3A	1.759(5)
N2A–C7A	1.375(6)
N3A–C12A	1.464(5)
N1A–C9A	1.327(6)
N1A–C1A	1.359(6)
C7A–N2A–H2AN	125(3)
C13A–N3A–C12A	119.7(4)
N3A–C13A–C14A	121.0(4)
O1A–C15A–C16A	118.5(4)
Fe1A–C31A–H31A	127.0
N3A–C13A–C14A–C19A	–176.4(4)
C19A–C18A–C20A–C21A	–178.0(4)

Table 1 and relevant crystallographic data and refinement parameters are given in Table 2. Crystals were grown by diffusion of petroleum ether into a solution of compound **6** in dichloromethane. The compound crystallised in the monoclinic $P2_1/c$ space group. Two molecules (**6A** and **6B**) were obtained and both of these structures are represented in the ESI.† All non-hydrogen atoms were refined anisotropically. In **6B** (Fig. S1†), atoms N2B, C10B, C11B and C12B were disordered over two positions. The site occupancies were refined to 0.616 for N2B, C10B, C11B and C12B, and 0.384 for N2C, C10C, C11C and C12C. These disordered atoms were refined with restrained anisotropic displacement parameters and their attached hydrogen atoms were excluded from the final model. The hydrogen atoms H1AO, H1BO and H2AN were positioned in different electron density maps and refined with restrained O–H or N–H bond lengths of 0.970 (5) Å. The remaining hydro-

Table 2 Crystal data and structure refinement for complex **6**

Empirical formula	$C_{31}H_{28}ClFeN_3O$ (A), $C_{31}H_{21}ClFeN_3O$ (B)
Formula weight	1092.67
Temperature (K)	173
Radiation (Å)	0.71073
Crystal system	Monoclinic
Space group	$P2_1/c$
Unit cell dimensions	
a (Å)	10.156(16)
b (Å)	40.86(7)
c (Å)	12.657(19)
α (°)	90
β (°)	90.276(17)
γ (°)	90
V (Å ³)	5252(15)
Z	4
Density (calculated) (g cm ⁻³)	1.382
$F(000)$	2260
Crystal size (mm)	0.03 × 0.09 × 0.12
Theta minimum–maximum (°)	1.7 to 25.2
Data set	–11 : 12; –48 : 38; –15 : 9
Total reflections	34 198
Unique reflections	9335 [$R(\text{int}) = 0.102$]
R indices	$R_1 = 0.0565$, $wR_2 = 0.1529$
Minimum and maximum res. dens. (eÅ ⁻³)	–0.66, 0.53

gen atoms were placed in idealised positions and refined in riding models with U_{iso} assigned 1.2 times U_{eq} of their parent atoms and the C–H bond distances were constrained to 0.95 or 0.99 Å.

Fig. 2 displays the molecular structure of **6A**, the geometry of the alkene moiety is thus confirmed. The alkenyl moiety adopts an *E* configuration which was corroborated by the coupling constants observed in the ¹H NMR spectrum. In addition to this, the imine C=N bond also adopts an *E* geometry, which is the most sterically favourable configuration. The Cp rings of the ferrocenyl entity adopt a near eclipsed conformation. The quinoline is connected to the salicylaldimine moiety *via* the propyl chain that displays a staggered arrangement. The quinoline ring appears to be oriented parallel to the plane of the salicylaldimine ring.

In vitro antiparasitic activity against *Plasmodium falciparum*

The antiplasmodial activity of compounds **1–16** were evaluated *in vitro* against two strains of *P. falciparum*, *i.e.* the NF54 (CQS) and K1 (CQR) strain in order to identify any effects of the polyamine scaffold, multinuclearity, amine functionalities and imine functionalities on antiplasmodial activity. CQ and FQ were used as reference drugs for comparison. The data obtained from this study are given in Table 3.

Generally, the monomeric ferrocenyl complexes (**6–8**) exhibit enhanced activities compared to the dimeric (**9–11**) and trimeric ferrocenyl (**12–14**) derivatives against both strains of the parasite. The quinoline precursors (**1–3**) generally display good activity in the sensitive strain with IC_{50} values

Table 3 *In vitro* antiplasmodial activity and resistance indices of compounds **1–16**, CQ and FQ against the NF54 CQ-sensitive and the K1 CQ-resistant strains of *P. falciparum*

Compound	$IC_{50}^a \pm SE$ NF54 ^b (μM)	$IC_{50} \pm SE$ K1 ^c (μM)	Resistance index (RI) ^d
1	0.0034 ± 0.013	1.819 ± 0.297	535
2	1.007 ± 0.065	7.179 ± 2.079	7.129
3	1.318 ± 0.293	20.75 ± 4.81	15.74
4	0.452 ± 0.0602	1.55 ± 0.090	3.43
5	21.36 ± 5.41	— ^e	—
6	0.040 ± 0.0091	0.951 ± 0.236	23.78
7	0.0318 ± 0.0056	1.985 ± 0.955	62.42
8	0.083 ± 0.01	0.59 ± 0.03	7.11
9	0.3621 ± 0.0748	3.066 ± 0.566	8.467
10	1.217 ± 0.0774	8.64 ± 1.09	7.099
11	0.72 ± 0.04	0.65 ± 0.04	0.90
12	2.479 ± 0.264	2.536 ± 0.662	1.023
13	2.219 ± 0.087	2.013 ± 0.547	0.907
14	0.647 ± 0.0678	0.646 ± 0.175	0.998
15	0.0732 ± 0.0061	0.3387 ± 0.0568	4.63
16	0.064 ± 0.0031	0.1748 ± 0.00532	2.73
CQ	0.0078 ± 0.002	0.30 ± 0.038	38
FQ	0.033 ± 0.01	0.014 ^f	0.42

^a IC_{50} represents the micromolar equivalents required to inhibit parasite growth by 50%. ^b NF54 chloroquine-sensitive strain of *P. falciparum*. ^c K1 chloroquine-resistant strain of *P. falciparum*. ^d Resistance index (RI) = $IC_{50}K1/IC_{50}NF54$. ^e Not determined. ^f Literature value.¹⁹



ranging between 0.0034 and 1.318 μM , with **1** showing activity comparable to CQ. The compounds exhibit a similar activity profile to CQ, with the compounds losing activity in the K1 strain compared to the NF54 strain. Incorporating ferrocene as part of these systems appears to improve the activity in the CQR strain. The resistance indices (RI) were calculated for the compounds, where applicable, and it was observed that the monomers display larger RI values compared to the dimeric and trimeric derivatives with the trimeric ferrocenes (**12–14**) exhibiting RI values close to 1. Complex **11** also exhibits a RI value of 0.9. This suggests that incorporation of the polyamine backbone (specifically the DAB scaffold) is beneficial for maintaining or enhancing activity in the resistant strain. Overall it appears that the ferrocenyl derivatives (**8**, **11**, and **14**), which do not possess the salicyl- and benzyl-moieties, exhibit the best activity profiles across the two strains. For example, complex **8** exhibits a lower RI value compared to monomers **6** and **7**. Complexes **11** and **14** gave resistance index values of 0.907 and 0.998, respectively and also demonstrated IC_{50} values lower than 1 μM . These results are promising despite the compounds being slightly less active than CQ.

When comparing the activity of imines (**6** and **8**) to the activity of the corresponding amines (**15** and **16**, respectively), there appears to be no significant difference in activity in the CQS strain between the corresponding imines and amines. There does however, appear to be a noticeable enhancement in activity in the K1 strain for the amines, thus resulting in lower RI values. This is also further supported by the synthesis of the amino versions of the trimeric derivatives instead of the imino-versions. All three trimeric compounds (**12–14**) exhibit good RI values, indicating that the compounds display consistent activity across both strains, possibly a consequence of their increased lipophilicity (Table 4) compared to the monomeric and dimeric complexes. Complex **14** is of particular interest

because in addition to the favourable RI value observed, the compound also exhibited promising antiplasmodial activity, giving an IC_{50} values of 0.65 μM in both strains of the *Plasmodium* parasite.

β -Haematin inhibition studies

Inhibition of haemozoin formation is a target for many quinoline-based compounds, including CQ.^{20,21} Quinolines inhibit haemozoin crystal growth in the digestive vacuole of the parasite. CQ, for example, is believed to bind to a toxic product of haemoglobin degradation called haematin (ferriprotoporphyrin IX). Quinoline-binding prevents conversion into haemozoin, which is less toxic to the parasite than haematin. Parasite damage occurs when there is a build-up of ferriprotoporphyrin IX, which ultimately leads to parasite death.^{20,21} β -Haematin is a synthetic form of haemozoin and inhibition of its synthesis can be studied using a NP-40 detergent-mediated assay.²² Haemozoin formation is not a spontaneous process and literature has shown that haem crystallisation occurs in the presence of neutral lipids inside of the digestive vacuole of the parasite.^{23,24} The concentration of unreacted haematin is quantified using a colorimetric pyridine ferrochrome method developed by Ncokazi and Egan.²⁵ The neutral detergent, NP-40, was used to mimic lipids and mediates β -haematin formation in the assay.

Compounds **3–16** were evaluated for their ability to inhibit β -haematin formation and the data is presented in Table 4. The degree of lipophilicity of these compounds was also predicted and is also depicted here. The DAB-derived quinoline precursor (**3**) exhibited moderate β -haematin inhibition with an IC_{50} value of 25.36 μM , while the ferrocenyl aldehydes (**4** and **5**) did not inhibit β -haematin formation at the tested concentration, suggesting that the quinoline motif is essential for inhibition. The monomeric ferrocenyl complexes **6–8** exhibited the weakest β -haematin inhibition of all of the tested compounds. These monomers display similar β -haematin inhibition when compared to CQ. The dimeric ferrocenyl complexes (**9–11**) were approximately twice as active as their monomeric counterparts. The IC_{50} values for these compounds were observed in the range of 23 to 48 μM . The salicyldimine derivative exhibited the best inhibition of the three dinuclear compounds. The lower values confirm that these compounds inhibit β -haematin crystallisation to a greater extent. Similarly, the trimeric ferrocenyl complexes (**12–14**) exhibit enhanced inhibition when compared to the monomeric and dimeric analogues. Increased lipophilicity may be a reason for this enhanced activity. The monomers (**6–8**) and dimers (**9–11**) are less lipophilic than **12–14**. In addition to this, amines **15** and **16** exhibit enhanced β -haematin inhibition compared to their corresponding imine derivatives (**6** and **8**). This alludes to some importance of the amine moiety as well as lipophilicity for activity. This is clearly evident when looking at the antiplasmodial activity. Enhanced lipophilicity and the presence of the amine appears to be beneficial for overcoming cross-resistance. Enhanced biological activity of multinuclear systems has been well documented in literature.^{8–10,26,27}

Table 4 β -Haematin inhibition values of **3–16** and CQ using the NP40 detergent-mediated assay

Compound	IC_{50}^a (μM)	95% confidence interval	$\log P^c$
3	25.36	16.61 to 38.71	0.67
4	>100	— ^b	4.93
5	>100	—	4.52
6	64.18	60.96 to 67.57	6.97
7	67.73	64.41 to 71.23	7.34
8	54.57	52.78 to 56.41	4.51
9	22.62	19.09 to 26.79	12.30
10	48.44	47.26 to 49.65	13.04
11	33.70	32.50 to 34.94	7.36
12	16.81	16.33 to 17.30	15.71
13	11.38	10.88 to 11.90	16.82
14	10.37	9.07 to 11.86	8.30
15	8.64	8.06 to 9.26	6.50
16	29.84	27.57 to 32.30	4.03
CQ	73.76	71.32 to 76.28	4.63 ^d

^a IC_{50} represents the micromolar equivalents required to inhibit β -haematin growth by 50%. ^b Not determined. ^c $\log P$ values predicted using MarvinSketch V5.9.4 (values do not take into account possible intramolecular H-bonding). ^d Literature value.¹⁷



In vitro antiparasitic activity against *T. vaginalis*

The synthesised compounds (1–16) were screened against the metronidazole-sensitive G3 strain of *T. vaginalis* at either 50 or 100 μM concentrations. The data obtained for this study are presented in Fig. 3 and Table 5.

The tested compounds exhibited various activity profiles against this particular parasite. The un-functionalised quinolines (1–3) and aldehydes (4–5) exhibited weak activity against the parasite. In most cases (with the exception of 12), compounds that possess the salicylaldimine or salicylaldamine moieties exhibit enhanced activity compared to the other derivatives. The amines (13–16) generally exhibit good activity. Amines 15 and 16 exhibit greater inhibition than their imine counterparts 6 and 8, respectively. Selected compounds were then further screened to obtain IC_{50} values. The most active compound was found to be complex 14, giving an IC_{50} value of 18.84 μM . The tested samples do not exhibit comparable IC_{50} values (Table 5) to metronidazole but the data does show that incorporation of ferrocene as part of these systems can lead to enhanced activity. This is consistent with data observed in a previous study.⁹ The presence of amino groups appear to be beneficial for activity and also incorporation of the salicylald-

imine or salicylaldamine moiety seems advantageous for increased activity against *T. vaginalis*.

In vitro cancer cytotoxicity

Selected compounds and CQ were also screened against WHCO1 oesophageal cancer cells, as a model system to determine the cytotoxicity of these compounds and to relate this to their antiplasmodial activity. Compounds 3, 5, 12 and 14 were not screened against this cell line due to limited solubility of the compounds in DMSO. The results obtained from this study is given in Table 6.

All of the tested compounds, with the exception of 15 and 16, show moderate to good cytotoxicity against the WHCO1 oesophageal cancer cell line. Generally, the dimeric ferrocenyl-imine complexes (9–11) exhibit lower cytotoxicity compared to the monomeric ferrocenyl-imine derivatives (6–8). The monomeric ferrocenyl-amines (15 and 16) display remarkably enhanced cytotoxicity than their imine counterparts (6 and 8, respectively) as well as any of the other tested compounds as can be seen by the low selectivity indices shown in Table 6. The incorporation of the amine moieties appear to greatly increase toxicity. The trimeric complex 13, exhibited moderate cytotoxicity, similar to CQ but lower SI values due to lower antiplasmodial activity. Chloroquine and other quinoline-based compounds have been screened as potential anticancer agents against breast tissue in the past and thus the data obtained is consistent with previous observations.²⁹ Most of the compounds exhibit higher cytotoxicity than cisplatin. This is consistent with data obtained for various quinoline-containing compounds.¹⁷ The antiplasmodial activity of the monomers

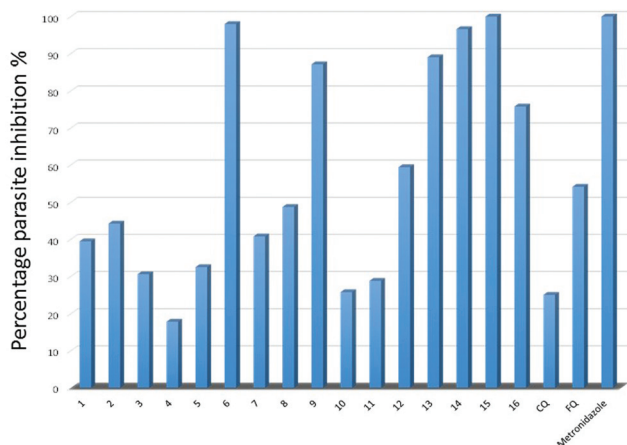


Fig. 3 *In vitro* antiparasitic activity of compounds 1–16, CQ, FQ, metronidazole against the G3 isolate of *T. vaginalis*.

Table 5 *In vitro* antiparasitic activity of selected against the G3 isolate of *T. vaginalis*

Compound	Percentage inhibition ^{a,b} % \pm SE	IC_{50} ^c (μM) \pm SE/SD*
6	97.97 \pm 7.13 ^a	24.53 \pm 0.08
9	87.10 \pm 3.39 ^a	22.21 \pm 0.03
14	96.60 \pm 2.99 ^b	18.84 \pm 1.22*
15	100 ^b	41.24 \pm 0.97*
Metronidazole	100 ^a	0.72

^a Parasite inhibition measured at 50 μM drug concentration. ^b Parasite inhibition measured at 100 μM drug concentration. ^c IC_{50} represents the micromolar equivalents required to inhibit parasite growth by 50%.

Table 6 Cytotoxicity of compounds 1–16, CQ and FQ against WHCO1 oesophageal cancer cells

Compound	IC_{50} ^a (μM)	95% Confidence interval	Selectivity index SI_1 ^d , SI_2 ^e
1	8.41	7.20 to 9.83	>100, 4.62
2	18.69	14.82 to 23.57	18.56, 2.60
3	— ^b	—	—
4	5.06	4.54 to 5.64	11.19, 3.26
5	—	—	—
6	1.97	1.56 to 2.50	49.25, 2.07
7	13.72	6.58 to 28.62	>100, 6.91
8	5.8	5.1 to 6.6	69.88, 9.83
9	9.01	8.02 to 10.11	24.88, 2.94
10	3.88	3.25 to 4.64	3.19, 0.45
11	8.0	7.2 to 9.0	11.11, 12.31
12	—	—	—
13	6.50	5.83 to 7.24	2.93, 2.56
14	—	—	—
15	0.31	0.26 to 0.36	4.23, 0.92
16	0.74	0.56 to 0.98	11.56, 4.23
CQ	6.3	5.7 to 6.9	>100, 21
FQ	17.3	13.1 to 22.8	>100, >100
Cisplatin	13.0 ^c	—	—

^a Values were determined from a dose response curve (assayed with MTT), IC_{50} represents the micromolar equivalents of test compounds required to produce 50% cell viability. ^b Not determined. ^c Literature value.²⁸ ^d SI_1 : IC_{50} WHCO1/ IC_{50} NF54. ^e SI_2 : IC_{50} WHCO1/ IC_{50} K1.



may be consequential of their toxicity and their ability to inhibit haemozoin formation, hence contributing to their enhanced activity compared to the polymeric structures in the malaria parasite. The dimeric complex **11** shows some promise as an antimicrobial agent as it exhibits some selectivity towards malarial parasites as can be seen by its SI values (>10) when examining both sensitive and resistant strains. This further supports the research of using polymeric systems as potential antiplasmodial agents, as these compounds may be less toxic towards mammalian cells and therefore more selective towards malarial parasites. More extensive studies are still required in order to establish a toxicity profile against various other human cell lines.

Normal flora bacterial cytotoxicity

To determine possible effects of these compounds on common normal flora bacteria, the entire library was screened on *Escherichia coli* K-12 MG1655, *Lactobacillus acidophilus* (ATCC 4356), *Lactobacillus rhamnosus* (ATCC 53103), and *Lactobacillus reuteri* (ATCC 23272) using the standard disc diffusion method.^{30,31} At the highest concentration tested (100 μM) no inhibitory activity was observed on any of these bacterial species. Similar tests on the pathogenic bacteria *Listeria monocytogenes* and *Salmonella enterica* show no inhibitory activity, indicating the selectivity of these compounds for eukaryotic pathogens and cancer.

Conclusions

A series of monomeric (**6–8**, **15–16**), dimeric (**9–11**) and trimeric (**12–14**) ferrocenyl quinoline complexes were prepared. All the compounds were characterised by a range of analytical and spectroscopic techniques. The compounds were evaluated for antiplasmodial activity against CQS and CQR *P. falciparum* strains. The trimeric complexes **12–14** displayed consistent activity across both strains, suggesting that the incorporation of the polyamine may be beneficial in overcoming cross-resistance. All of the quinoline-based derivatives were found to inhibit synthetic haemozoin formation and therefore may be the biological target of the complexes. The data suggests that enhancing the lipophilicity of the compounds as well as incorporating amino groups, positively affects the activity of the compounds in CQR strains. The complexes also exhibit moderate activity against the WHCO1 oesophageal cancer cell line with the monomeric amino complexes (**15** and **16**) exhibiting the highest toxicity. Data obtained for the G3 strain of *T. vaginalis* showed that the salicylaldehyde derived complexes (**6** and **9**) exhibit promising activity when screened at 50 μM drug concentration. The ferrocenyl-based quinolines, especially the multimeric derivatives, may be a feasible system to be researched as potential antiparasitic agents. Furthermore, the lack of cytotoxicity against normal flora bacteria suggests these compounds are selective against eukaryotic pathogens and cancer.

Experimental

General details

Synthetic procedures were performed under an argon atmosphere at ambient temperatures unless otherwise stated. All reagents were purchased from Sigma Aldrich and used as received. Solvents were dried over Fluka Molecular Sieves with indicator. Nuclear magnetic resonance (NMR) spectra were recorded on a Varian Unity XR400 spectrometer (^1H : 399.95 MHz, $^{13}\text{C}\{^1\text{H}\}$: 100.58 MHz), Varian Mercury XR300 spectrometer (^1H : 300.08 MHz, $^{13}\text{C}\{^1\text{H}\}$: 75.46 MHz) or Bruker Ultrashield 400 Plus spectrometer (^1H : 400.20 MHz, $^{13}\text{C}\{^1\text{H}\}$: 100.60 MHz) at 30.0 $^\circ\text{C}$ using tetramethylsilane (TMS) as the internal standard. Infrared (IR) absorptions were measured on a PerkinElmer Spectrum One FT-IR spectrometer and samples were analysed using attenuated total reflectance (ATR) or as KBr pellets. Elemental analyses were carried out using a Fisons EA 110 elemental analyser. The purity (>95%) of selected samples was checked using an analytical Agilent HPLC 1260 equipped with a Agilent DAD 1260 UV/vis detector and a X Bridge C18 column (2.5 μM , 50 mm \times 3 mm). The compounds were eluted using a mixture of solvent A (10 mM $\text{NH}_4\text{OAc}/\text{H}_2\text{O}$) and solvent B (10 mM $\text{NH}_4\text{OAc}/\text{MeOH}$) at a flow rate of 0.9 mL min^{-1} . The gradient elution conditions were as follows: 10% solvent B between 0–1 min, 10–95% solvent B between 1–3 min, 95% solvent B between 3–5 min. High resolution (HR) ESI-mass spectrometry was used to further characterise all new compounds and determinations were carried out using a Waters API Quattro instrument in the positive mode. The precursors, *N*-(7-chloroquinolin-4-yl)propane-1,3-diamine (**1**),¹³ *N*-(7-chloroquinolin-4-yl) tris(2-aminoethyl)amine (**2**),¹⁴ ferrocene benzaldehyde (**5**)^{15,16} and quinoline ferrocenylamine (**16**)¹⁸ were synthesized following literature methods.

Synthesis of compounds

***N*-(7-Chloroquinolin-4-yl)-tetrakis(3-aminopropyl)-1,4-butanedi-amine (3)**. 4,7-Dichloroquinoline (0.250 g, 1.26 mmol) and the G1 DAB dendrimer (5 ml) were stirred together at 90 $^\circ\text{C}$ for 18 hours. Upon cooling, 1 M NaOH (10 ml) was added. The aqueous extracts were washed with dichloromethane (3 \times 50 ml). This was then washed with water (1 \times 10 ml). The organic phase was collected and dried over Na_2SO_4 . The drying agent was removed by filtration and the solvent removed *in vacuo* to give rise to the product (**3**) as a yellow oil (90.3 mg, 15%). ^1H NMR (300.08 MHz, $\text{DMSO}-d_6$): (δ , ppm) 1.35–1.50 (10H, m, CH_2/NH_2); 1.53–1.68 (6H, m, CH_2); 1.84 (2H, m, CH_2); 2.30–2.58 (12H, m, CH_2); 2.64–2.78 (6H, m, CH_2); 3.25–3.33 (2H, m, CH_2); 6.45 (1H, d, $^3J_{\text{H-H}} = 5.49$, ArH); 7.44 (1H, dd, $^4J_{\text{H-H}} = 2.19$, $^3J_{\text{H-H}} = 8.97$, ArH); 7.77 (1H, d, $^4J_{\text{H-H}} = 2.19$, ArH); 8.24 (1H, d, $^3J_{\text{H-H}} = 8.91$, ArH); 8.39 (1H, d, $^3J_{\text{H-H}} = 5.43$, ArH). IR (ATR): ($\nu_{\text{max}}/\text{cm}^{-1}$) 1609. ESI-MS: m/z 520.3339 ($[\text{M} + \text{CH}_3\text{CN} + \text{H}]^+$). HPLC $t_{\text{R}} = 0.55$ min.

Ferrocene-salicylaldehyde (4). 5-Iodosalicylaldehyde (0.257 g, 1.04 mmol), vinylferrocene (0.536 g, 2.53 mmol), tri(*p*-tolyl)phosphine (33.9 mg, 0.111 mmol), $\text{Pd}(\text{OAc})_2$ (16.3 mg,



0.0726 mmol) and Et₃N (0.5 ml) were reacted in acetonitrile (10 ml) at 90 °C for 24 hours. The solvent was then removed *in vacuo*. The residue was dissolved in DCM and the organic fraction washed with water (2 × 10 ml). The organic layer was collected and dried over MgSO₄. The crude material was purified using column chromatography using EtOAc and petroleum ether as the eluent (1 : 50). The product (**4**) was obtained as a dark red solid (0.132 g, 38%). ¹H NMR (300.08 MHz, CDCl₃): (δ, ppm) 4.20 (5H, s, Cp); 4.36 (2H, s, Cp); 4.53 (2H, s, Cp); 6.59 (1H, d, ³J_{H-H} = 16.23, -C=CH); 6.76 (1H, d, ³J_{H-H} = 15.66, -C=CH); 6.97 (1H, d, ³J_{H-H} = 8.61, ArH); 7.54 (1H, s, ArH); 7.61 (1H, d, ³J_{H-H} = 8.37, ArH); 9.92 (1H, s, COH); 10.94 (1H, s, OH). ¹³C{¹H} NMR (100.635 MHz, CDCl₃): 66.80; 69.09; 69.22; 83.07; 118.00; 120.64; 123.97; 126.47; 130.41; 130.56; 134.06; 160.51; 196.58. IR (ATR): (ν_{max}/cm⁻¹) 1653; 1581. EI-MS: *m/z* 332.0513 ([M]⁺, requires 332.0499). HPLC *t*_R = 5.42 min.

Mono-salicyldimine ferrocenyl quinoline (6). *N*-(7-Chloroquinolin-4-yl)-propane-1,3-diamine (**1**) (62.1 mg, 0.263 mmol) and the aldehyde (**4**) (88.6 mg, 0.267 mmol) were stirred in a DCM-MeOH (1 : 1, v/v) mixture (30 ml). The resulting solution was stirred at room temperature for 24 hours. The solvent was then reduced and the product precipitated with petroleum ether. The product was filtered and dried *in vacuo*. Further purification was achieved by stirring the suspended solid in petroleum ether to remove any unreacted aldehyde. The product (**6**) was isolated as an orange powder (0.145 g, 85%). ¹H NMR (300.077 MHz, CDCl₃): (δ, ppm) 2.16–2.25 (2H, m, CH₂); 3.45–3.52 (2H, m, CH₂); 3.80 (2H, t, ³J_{H-H} = 6.03, CH₂); 4.13 (5H, s, Cp); 4.26 (2H, t, ³J_{H-H} = 1.86, Cp); 4.43 (2H, t, ³J_{H-H} = 1.92, Cp); 5.06 (1H, t, ³J_{H-H} = 4.95, NH); 6.42 (1H, d, ³J_{H-H} = 5.40, ArH); 6.62 (1H, d, ³J_{H-H} = 16.11, -C=CH); 6.72 (1H, d, ³J_{H-H} = 16.14, -C=CH); 6.97 (1H, d, ³J_{H-H} = 8.52, ArH); 7.25 (1H, d, ⁴J_{H-H} = 2.19, ArH); 7.31 (1H, dd, ⁴J_{H-H} = 2.13, ³J_{H-H} = 8.91, ArH); 7.45 (1H, dd, ⁴J_{H-H} = 2.19, ³J_{H-H} = 8.61, ArH); 7.62 (1H, d, ³J_{H-H} = 8.88, ArH); 7.95 (1H, d, ⁴J_{H-H} = 2.19, ArH); 8.40 (1H, s, HC=N-); 8.53 (1H, d, ³J_{H-H} = 5.34, ArH); 13.20 (1H, s, OH). ¹³C{¹H} NMR (100.635 MHz, CDCl₃): 29.99; 41.40; 57.44; 66.66; 68.88; 69.16; 83.60; 99.15; 117.15; 117.42; 118.55; 120.76; 124.94; 125.05; 125.42; 128.68; 128.92; 129.30; 129.86; 134.92; 149.20; 149.47; 152.06; 160.09; 165.82. IR (ATR): (ν_{max}/cm⁻¹) 1634; 1613; 1580. Elemental Analysis C₃₁H₂₈ClFeN₃O·0.3H₂O calculated: C 67.05; H 5.19%, found: C 67.20; H 5.69%. ESI-MS: *m/z* 550.1336 ([M + H]⁺, requires 550.1348).

Mono-benzaldimine ferrocenyl quinoline (7). *N*-(7-Chloroquinolin-4-yl)-propane-1,3-diamine (**1**) (79.2 mg, 0.336 mmol) and the aldehyde (**5**) (0.108 g, 0.343 mmol) were stirred in a DCM-MeOH (1 : 1, v/v) mixture (30 ml). The resulting solution was stirred at room temperature for 24 hours. The solvent was then reduced and the product precipitated with petroleum ether. The product was filtered and dried *in vacuo*. Further purification was achieved by stirring the suspended solid in petroleum ether to remove any unreacted aldehyde. The product (**7**) was isolated as an orange powder (96.6 mg, 54%). ¹H NMR (300.08 MHz, CDCl₃): (δ, ppm) 2.14–2.22 (2H, m,

CH₂); 3.49–3.54 (2H, m, CH₂); 3.85 (2H, t, ³J_{H-H} = 5.79, CH₂); 4.19 (5H, s, Cp); 4.36 (2H, t, ³J_{H-H} = 1.83, Cp); 4.54 (2H, t, ³J_{H-H} = 1.92, Cp); 6.41 (1H, d, ³J_{H-H} = 5.31, ArH); 6.46 (1H, t, ³J_{H-H} = 4.23, NH); 6.77 (1H, d, ³J_{H-H} = 16.14, -C=CH); 7.04 (1H, d, ³J_{H-H} = 16.11, -C=CH); 7.23 (1H, dd, ⁴J_{H-H} = 2.19, ³J_{H-H} = 8.97, ArH); 7.53 (2H, d, ³J_{H-H} = 8.25, ArH); 7.71–7.76 (3H, m, H-5, ArH); 7.96 (1H, d, ⁴J_{H-H} = 2.10, ArH); 8.34 (1H, s, HC=N-); 8.54 (1H, d, ³J_{H-H} = 5.31, ArH). ¹³C{¹H} NMR (100.635 MHz, CDCl₃): 29.60; 43.41; 60.83; 67.15; 69.32; 69.43; 82.77; 98.69; 117.34; 121.74; 124.94; 125.06; 125.99; 128.49; 128.62; 129.36; 134.06; 134.81; 140.89; 148.93; 150.24; 151.90; 161.90. IR (ATR): (ν_{max}/cm⁻¹) 1639; 1629; 1602. Elemental Analysis C₃₁H₂₈ClFeN₃·0.2CH₂Cl₂ calculated: C 68.03; H 5.20%, found: C 68.47; H 4.70%. ESI-MS: *m/z* 534.1394 ([M + H]⁺, requires 534.1399). HPLC *t*_R = 5.36 min.

Mono-ferrocenyl quinoline (8). To a suspension of *N*'-(7-Chloroquinolin-4-yl)-propane-1,3-diamine **1** (0.203 g, 0.862 mmol) in diethyl ether (30 ml), a solution of ferrocenecarboxaldehyde (0.204 g, 0.952 mmol) in diethyl ether (5 ml) was added and the mixture stirred for 16 hours at room temperature. An orange precipitate was filtered, washed with diethyl ether to remove excess aldehyde and the solid dried *in vacuo*. Compound **8** was obtained as an orange powder (0.310 g, 83%). ¹H NMR (399.951 MHz, CDCl₃): (δ, ppm) 2.06–2.14 (2H, m, CH₂); 3.44–3.48 (2H, m, CH₂); 3.70 (2H, t, ³J_{H-H} = 5.49, CH₂); 4.18 (5H, s, Cp); 4.46 (2H, t, ³J_{H-H} = 1.83, Cp); 4.69 (2H, t, ³J_{H-H} = 1.83, Cp); 6.36 (1H, d, ³J_{H-H} = 5.49, H-3); 6.76 (1H, br s, NH); 7.26 (1H, dd, ⁴J_{H-H} = 1.83, ³J_{H-H} = 8.79, ArH); 7.80 (1H, d, ³J_{H-H} = 8.79, ArH); 7.93 (1H, d, ⁴J_{H-H} = 2.19, ArH); 8.18 (1H, s, HC=N-); 8.50 (1H, d, ³J_{H-H} = 5.13, ArH). ¹³C{¹H} NMR (100.635 MHz, CDCl₃): (δ, ppm) 29.68; 43.57; 61.32; 68.50; 69.16; 70.78; 80.31; 98.57; 117.49; 122.07; 124.83; 128.63; 134.66; 149.20; 150.27; 152.17; 162.00. IR (KBr): (ν_{max}/cm⁻¹) 3274; 1638; 1613. Elemental Analysis C₂₃H₂₂ClFeN₃·2H₂O calculated: C 59.06; H 5.60%, found: C 59.21; H 4.92%. ESI-MS: *m/z* 432.0937 ([M + H]⁺, requires 432.0929).

Bis-salicyldimine ferrocenyl quinoline (9). *N*-(7-Chloroquinolin-4-yl) tris(2-aminoethyl)amine (**2**) (35.4 mg, 0.115 mmol) and the aldehyde (**4**) (79.2 mg, 0.230 mmol) were stirred in a DCM-MeOH (1 : 1, v/v) mixture (30 ml). The resulting solution was stirred at room temperature for 24 hours. After the 24 hour period, the solvent was reduced and the product precipitated with petroleum ether. The product was filtered and dried *in vacuo*. Further purification was achieved by stirring the suspended solid in petroleum ether to remove any unreacted aldehyde. The product (**9**) was isolated as an orange powder (32.1 mg, 30%). ¹H NMR (300.08 MHz, CDCl₃): (δ, ppm) 2.90–2.95 (6H, m, CH₂); 3.35 (2H, br s, CH₂); 3.63 (4H, br s, CH₂); 4.13 (10H, s, Cp); 4.27 (4H, s, Cp); 4.44 (4H, s, Cp); 6.15 (1H, br s, NH); 6.29–6.34 (1H, m, ArH); 6.49 (2H, d, ³J_{H-H} = 16.14, -C=CH); 6.56–6.64 (3H, m, H-6, -C=CH); 6.71 (2H, d, ³J_{H-H} = 8.25, ArH); 6.86 (2H, s, ArH); 7.19 (2H, d, ³J_{H-H} = 8.16, ArH); 7.31 (2H, d, ³J_{H-H} = 8.34, ArH); 7.88 (1H, br s, ArH); 8.15 (2H, s, HC=N-); 8.42 (1H, br s, ArH); 13.60 (2H, s, OH). ¹³C{¹H} NMR (100.635 MHz, CDCl₃): (δ, ppm) 40.49; 52.69; 55.17; 56.71; 66.74; 68.82; 69.18; 83.80; 98.64; 117.15; 117.54;



117.95; 121.54; 124.99 (2C); 125.85; 128.88; 128.99; 129.89; 135.79; 146.73; 161.14; 166.05. IR (ATR): ($\nu_{\max}/\text{cm}^{-1}$) 1633; 1611; 1583. Elemental Analysis $\text{C}_{53}\text{H}_{50}\text{ClFe}_2\text{N}_5\text{O}_2 \cdot 3\text{H}_2\text{O}$ calculated: C 64.29; H 5.70%, found: C 64.49; H 5.39%. ESI-MS: m/z 936.2441 ($[\text{M} + \text{H}]^+$, requires 936.2430).

Bis-benzaldimine ferrocenyl quinoline (10). *N*-(7-Chloroquinolin-4-yl) tris(2-aminoethyl)amine (2) (93.9 mg, 0.305 mmol) and the aldehyde (5) (192 mg, 0.607 mmol) were stirred in a DCM–MeOH (1 : 1, v/v) mixture (30 ml). The resulting solution was stirred at room temperature for 24 hours. The solvent was then reduced and the product precipitated with petroleum ether. The product was filtered and dried *in vacuo*. Further purification was achieved by stirring the suspended solid in *n*-pentane to remove any unreacted aldehyde. The product (10) was isolated as a red powder (58.1 mg, 21%). ^1H NMR (300.08 MHz, CDCl_3): (δ , ppm) 2.99–3.05 (6H, m, CH_2); 3.32–3.36 (2H, m, CH_2); 3.76 (4H, t, $^3J_{\text{H-H}} = 5.58$, CH_2); 4.18 (10H, s, Cp); 4.33 (4H, t, $^3J_{\text{H-H}} = 1.74$, Cp); 4.44 (4H, t, $^3J_{\text{H-H}} = 1.92$, Cp); 6.28 (1H, br s, NH); 6.36 (1H, d, $^3J_{\text{H-H}} = 5.41$, ArH); 6.63–6.72 (3H, m, $-\text{C}=\text{CH}$, ArH); 6.95 (2H, d, $^3J_{\text{H-H}} = 16.32$, $-\text{C}=\text{CH}$); 7.29–7.35 (4H, m, ArH); 7.47 (4H, d, $^3J_{\text{H-H}} = 8.46$, ArH); 7.86 (1H, d, $^4J_{\text{H-H}} = 2.28$, ArH); 8.20 (2H, s, $\text{HC}=\text{N}$); 8.50 (1H, d, $^3J_{\text{H-H}} = 5.52$, ArH). $^{13}\text{C}\{^1\text{H}\}$ NMR (100.635 MHz, CDCl_3): (δ , ppm) 40.53; 53.01; 55.64; 60.29; 67.12; 69.30 (2C); 82.96; 99.08; 117.48; 121.66; 125.07; 125.25; 125.80; 128.09; 128.44; 128.92; 130.32; 134.11; 140.46; 148.93; 150.13; 151.80; 161.81. IR (ATR): ($\nu_{\max}/\text{cm}^{-1}$) 1632; 1600. Elemental Analysis $\text{C}_{53}\text{H}_{50}\text{ClFe}_2\text{N}_5$ calculated: C 70.40; H 5.57%, found: C 70.04; H 5.24%. ESI-MS: m/z 904.2499 ($[\text{M} + \text{H}]^+$, requires 904.2532).

Bis-ferrocenyl quinoline (11). *N*-(7-Chloroquinolin-4-yl)-tris(2-aminoethyl)amine (2) (0.144 g, 0.469 mmol) was dissolved in EtOH (25 ml). To this, ferrocenecarboxaldehyde (0.200 g, 0.935 mmol) in EtOH (5 ml) was added and the resulting solution stirred at room temperature for 16 hours. The solvent was then removed *in vacuo* and the residue washed continuously with *n*-pentane. The product (11) was isolated as an orange-brown powder (0.102 g, 31%). ^1H NMR (399.951 MHz, CDCl_3): (δ , ppm) 2.91 (4H, t, $^3J_{\text{H-H}} = 5.49$, CH_2); 2.99 (2H, t, $^3J_{\text{H-H}} = 5.13$, CH_2); 3.29–3.33 (2H, m, CH_2); 3.59 (4H, t, $^3J_{\text{H-H}} = 5.86$, CH_2); 4.31 (10H, s, Cp); 4.29 (4H, br s, Cp); 4.50 (4H, br s, Cp); 6.33 (1H, d, $^3J_{\text{H-H}} = 5.13$, ArH); 6.66 (1H, br s, NH); 7.07 (1H, d, $^3J_{\text{H-H}} = 8.42$, ArH); 7.70 (1H, d, $^3J_{\text{H-H}} = 8.79$, ArH); 7.89 (1H, s, ArH); 8.10 (2H, s, $\text{HC}=\text{N}$); 8.48 (1H, d, $^3J_{\text{H-H}} = 5.13$, ArH). $^{13}\text{C}\{^1\text{H}\}$ NMR (100.635 MHz, CDCl_3): (δ , ppm) 41.11; 53.19; 55.95; 60.89; 68.48; 69.05; 70.47; 80.31; 99.01; 117.78; 122.35; 125.18; 128.31; 134.54; 149.22; 150.37; 151.95; 162.04. IR (KBr): ($\nu_{\max}/\text{cm}^{-1}$) 3267; 1639; 1611. Elemental Analysis $\text{C}_{37}\text{H}_{38}\text{ClFe}_2\text{N}_5 \cdot 4\text{H}_2\text{O}$ calculated: C 57.57; H 6.01%, found: C 57.46; H 4.54%. ESI-MS (HR): m/z 700.1611 (100%, $[\text{M} + \text{H}]^+$, requires 700.1593). HPLC $t_{\text{R}} = 3.66$ min.

General procedure for the preparation of tris-ferrocenyl quinolines

To a solution of compound 3 (1 eq.) in MeOH (10 ml), a solution of the aldehyde (3 eq.) in DCM (10 ml) was added. The solution was stirred in the presence of molecular sieves for

16 hours at room temperature. The molecular sieves were then removed by filtration and the filtrate collected. The solvent was removed *in vacuo*. *n*-Pentane was added and the residue was stirred and the solvent decanted. This was repeated several times until the supernatant remained clear. The remaining solid was then dissolved in DCM (20 ml), NaBH_4 was suspended and MeOH (5 ml) was then added. The reaction mixture was then allowed to stir for 6 hours at room temperature. After this time, water was added and the mixture placed in a separating funnel. The organic layer was then washed with water (2×10 ml), the organic layer was collected and dried over MgSO_4 . The drying agent was then removed by filtration, the filtrate collected and the solvent reduced *in vacuo*. The products were precipitated with petroleum ether.

Tris-salicylaldimine ferrocenyl quinoline (12). To a solution of compound 3 (47.7 mg, 0.0997 mmol) in MeOH, a solution of the aldehyde 4 (99.4 mg, 0.299 mmol) in DCM was added. To the intermediate, NaBH_4 (15.6 mg, 0.412 mmol) was added to afford the desired amine. The product was afforded as a dark brown solid (12) (0.112 g, 79%). ^1H NMR (300.08 MHz, CDCl_3): (δ , ppm) 1.20–1.94 (12H, m, CH_2); 2.30–2.76 (20H, m, CH_2); 3.30–3.35 (2H, m, CH_2); 3.83–3.99 (4H, m, CH_2); 4.14 (15H, s, Cp); 4.26 (6H, br s, Cp); 4.43 (6H, br s, Cp); 6.32 (1H, d, $^3J_{\text{H-H}} = 5.31$, ArH); 6.58–6.71 (6H, m, $\text{HC}=\text{CH}$); 6.78 (3H, d, $^3J_{\text{H-H}} = 8.25$, ArH); 6.99–7.07 (4H, m, ArH); 7.20–7.37 (4H, m, ArH); 7.59–7.73 (1H, m, ArH); 7.91–7.96 (1H, m, ArH); 8.51 (1H, d, $^3J_{\text{H-H}} = 6.51$, ArH). IR (ATR): ($\nu_{\max}/\text{cm}^{-1}$) 1607; 1580. Elemental Analysis $\text{C}_{82}\text{H}_{92}\text{ClFe}_3\text{N}_7\text{O}_3 \cdot 4\text{H}_2\text{O}$ calculated: C 65.72; H 6.73%, found: C 65.66; H 6.26%. ESI-MS (HR): m/z 713.7587 ($[\text{M} + 2\text{H}]^{2+}$, requires 713.7572); 476.1762 ($[\text{M} + 3\text{H}]^{3+}$, requires 476.1739).

Tris-benzaldimine ferrocenyl quinoline (13). To a solution of compound 3 (68.3 mg, 0.143 mmol) in MeOH, a solution of the aldehyde 5 (136 mg, 0.429 mmol) in DCM was added. To the imine, NaBH_4 (23.7 mg, 0.626 mmol) was added to afford the desired amine. The product was afforded as an orange powder (13) (81.7 mg, 41%). ^1H NMR (300.08 MHz, CDCl_3): (δ , ppm) 1.21–1.96 (12H, m, CH_2); 2.29–2.82 (20H, m, CH_2); 3.30–3.37 (2H, m, CH_2); 3.73–3.81 (4H, m, CH_2); 4.12–4.18 (15H, m, Cp); 4.28–4.31 (6H, m, Cp); 4.45–4.48 (6H, m, Cp); 6.31 (1H, d, $^3J_{\text{H-H}} = 5.43$, ArH); 6.65–8.88 (6H, m, $\text{HC}=\text{CH}$); 7.21–7.56 (14H, m, ArH, NH); 7.77 (1H, d, $^3J_{\text{H-H}} = 9.00$, ArH); 7.96 (1H, d, $^3J_{\text{H-H}} = 2.01$, ArH); 8.50 (1H, d, $^3J_{\text{H-H}} = 5.34$, ArH). IR (ATR): ($\nu_{\max}/\text{cm}^{-1}$) 1633; 1609; 1579. Elemental Analysis $\text{C}_{82}\text{H}_{92}\text{ClFe}_3\text{N}_7 \cdot 3\text{H}_2\text{O}$ calculated: C 68.74; H 6.89%, found: C 68.64; H 6.59%. ESI-MS (HR): m/z 1420.7250 ($[\text{M} + \text{CH}_3\text{CN} + \text{H}]^+$, requires 1420.7268).

Tris-ferrocenyl quinoline (14). To a solution of compound 3 (78.3 mg, 0.164 mmol) in MeOH, a solution of ferrocenecarboxaldehyde (106 mg, 0.496 mmol) in DCM was added. To the imine, NaBH_4 (28.9 mg, 0.764 mmol) was added to afford the desired amine. The product was afforded as a brown powder (14) (82.4 mg, 47%). ^1H NMR (300.08 MHz, CDCl_3): (δ , ppm) 1.25–1.97 (12H, m, CH_2); 2.22–2.74 (20H, m, CH_2); 3.28–3.57 (6H, m, CH_2); 4.00–4.39 (27H, m, Cp); 6.32 (1H, d, $^3J_{\text{H-H}} = 5.13$,



ArH); 7.31–7.38 (1H, m, ArH); 7.58–7.64 (1H, m, NH); 7.75 (1H, d, $^3J_{H-H}$ = 8.88, ArH); 7.95 (1H, d, $^3J_{H-H}$ = 1.86, ArH); 8.51 (1H, d, $^3J_{H-H}$ = 5.22, ArH). IR (ATR): ($\nu_{\max}/\text{cm}^{-1}$) 1611; 1579. Elemental Analysis $\text{C}_{58}\text{H}_{74}\text{ClFe}_3\text{N}_7 \cdot 3.5\text{H}_2\text{O}$ calculated: C 61.36; H 7.19%, found: C 61.13; H 7.01%. ESI-MS (HR): m/z 1072.3861 ($[\text{M} + \text{H}]^+$, requires 1072.3815).

Mono-salicyldamine ferrocenyl quinoline (15). To a solution of compound **6** (34.7 mg, 0.0631 mmol) in DCM (20 ml), to this, NaBH_4 (5.50 mg, 0.145 mmol) was suspended. Following this, MeOH (5 ml) was added to the reaction mixture. The reaction mixture was then allowed to stir for 6 hours at room temperature. Water was then added and the mixture placed in a separating funnel. The organic layer was then washed with water (2×10 ml). The organic layer was collected and dried over MgSO_4 . The drying agent was removed, the filtrate collected and the solvent removed *in vacuo* to give rise to an orange solid (**15**) (28.9 mg, 83%). ^1H NMR (300.08 MHz, CDCl_3): (δ , ppm) 1.92–2.03 (2H, m, CH_2); 2.84–2.91 (2H, m, CH_2); 3.42–3.51 (2H, m, CH_2); 4.07 (2H, s, CH_2); 4.14 (5H, s, Cp); 4.27 (2H, br s, Cp); 4.44 (2H, br s, Cp); 5.77 (1H, br s, NH); 6.37 (1H, d, $^3J_{H-H}$ = 3.48, ArH); 6.62 (1H, d, $^3J_{H-H}$ = 16.20, $-\text{C}=\text{CH}$); 6.71 (1H, d, $^3J_{H-H}$ = 16.14, $-\text{C}=\text{CH}$); 6.88 (1H, d, $^3J_{H-H}$ = 8.07, ArH); 7.10–7.14 (1H, m, ArH); 7.25–7.33 (1H, m, ArH); 7.61 (1H, d, $^3J_{H-H}$ = 8.25, ArH); 7.92 (1H, s, ArH); 8.46–8.51 (1H, m, ArH). $^{13}\text{C}\{^1\text{H}\}$ NMR (100.635 MHz, CDCl_3): (δ , ppm) 28.08; 40.95; 46.08; 52.63; 66.58; 68.75; 69.14; 83.95; 98.80; 116.61; 117.15; 121.38; 122.49; 124.21; 125.36; 125.72; 126.26; 126.42; 128.23; 129.67; 135.04; 148.65; 149.77; 151.46; 156.94. Elemental Analysis $\text{C}_{31}\text{H}_{30}\text{ClFeN}_3\text{O} \cdot \text{H}_2\text{O}$ calculated: C 65.33; H 5.66%, found: C 65.48; H 5.78%. ESI-MS: m/z 552.1 ($[\text{M} + \text{H}]^+$). HPLC t_R = 4.19 min.

Antiplasmodial assay

Samples were screened in triplicate on one occasion against the chloroquine-sensitive NF54 strain and chloroquine-resistant K1 strains of *Plasmodium falciparum*. Continuous *in vitro* cultures of asexual erythrocyte stages of *P. falciparum* were maintained using a modified version of the method of Trager and Jensen.³² Quantitative assessment of antiplasmodial activity *in vitro* was determined *via* the parasite lactate dehydrogenase assay using a modified method of that described by Makler *et al.*³³ The samples were prepared as a 20 mg ml^{-1} stock solution using DMSO and sonicated to enhance solubility. Samples were tested as a suspension if not completely dissolved. Stock solutions were stored at -20 °C. Further dilutions were prepared on the day of the experiment. Chloroquine was used as the reference drug in all experiments. A full dose–response measurement was performed for all compounds to determine the concentration inhibiting 50% of parasite growth (IC_{50} value). The samples were tested at a starting concentration of 1000 ng ml^{-1} , which was then serially diluted 2-fold in complete medium to give 10 concentrations; with the lowest concentration being approximately 2 ng ml^{-1} . The same dilution technique was used for all samples. The highest concentration of solvent to which the parasites were exposed to had no measurable effect on the parasite viability.

The IC_{50} values were obtained using a non-linear dose–response curve fitting analysis *via* Graph Pad Prism v.4.0 software.

Cytotoxicity (MTT) assay

The oesophageal cancer cell line WHCO1, derived from a primary oesophageal squamous cell carcinoma, was provided by Professor Rob Veale (University of the Witwatersrand, Johannesburg, South Africa). IC_{50} determinations were carried out using an MTT (3-(4,5-dimethylthiazol-2-yl)-2,5-diphenyltetrazolium bromide) assay.³⁴ 3000 cells were seeded per well in 96-well plates. Plates were incubated at 37 °C under 5% CO_2 (24 hours), after which aqueous DMSO solutions of each compound (10 μL , with a constant final concentration of DMSO of 0.2%) were plated at various concentrations. After 48 hours incubation, observations were made, and MTT (10 μL) solution added to each well. After 4 hours of incubation, solubilisation solution (100 μL) was added to each well, and incubated overnight. Plates were read at 595 nm on a BioTek microplate reader, and IC_{50} values calculated using Graph Pad Prism v.4.0. Package of GraphPad Software, San Diego, USA.

Antitrichomonal assay

Cultures of *T. vaginalis* G3 isolate were grown in 5 ml complete TYM Diamond's media in a 37 °C incubator for 24 hours. 50 mM stock solutions of the compounds were made in DMSO and were screened. Cells untreated and inoculated with 5 μL DMSO were used as controls. 5 μL of 50 mM stocks of compound library were inoculated for a final concentration of 50 μM . Results were calculated based on counts utilising a haemocytometer after 24 hours. The IC_{50} values were obtained using a non-linear dose–response curve fitting analysis *via* Graph Pad Prism v.5.0 software. All predicted IC_{50} values were confirmed using the same assay described above.

β -Haematin inhibition assay

The β -haematin assay was adapted from the method described by Wright and co-workers.²² Compounds were prepared as a 10 mM stock solution in 100% DMSO. Samples were tested at a starting concentration of 500 μM and the lowest drug concentration was 5 μM . The stock solution was serially diluted to give 12 concentrations in a 96 well flat-bottom assay plate. NP-40 detergent was then added to mediate the formation of β -haematin (30.55 μM , final concentration). A 25 mM stock solution of haematin was prepared by dissolving hemin (16.3 mg) in dimethyl sulfoxide (1 ml). A 177.76 μL aliquot of haematin stock was suspended in 20 ml of a 2 M acetate buffer, pH 4.7. The haematin suspension was then added to the plate to give a final haematin concentration of 100 μM . The plate was then incubated for 16 hours at 37 °C. The assay was analysed using the pyridineferrochrome method developed by Ncokazi and Egan.²³ 32 μL of a solution of 50% pyridine, 20% acetone, 20% water, and 10% 2 M HEPES buffer (pH 7.4) was added to each well. To this, 60 μL acetone was then added to each well and mixed. The absorbance of the resulting complex was measured at 405 nm on a SpectraMax



340PC plate reader. The IC₅₀ values were obtained using a non-linear dose–response curve fitting analysis *via* Graph Pad Prism v.5.0 software.

Disc diffusion antibiotic sensitivity assays for normal flora and pathogenic bacteria

Single colonies of common normal flora bacteria *Escherichia coli* K-12 MG1655, *Lactobacillus acidophilus* (ATCC 43560), *Lactobacillus rhamnosus* (ATCC 53103), and *Lactobacillus reuteri* (ATCC 23272) were inoculated into appropriate medium [Luria Broth (LB), Brain Heart Infusion Broth (BHI), or Lactobacilli MRS broth] and grown at 37° overnight with *Lactobacilli* strains grown under anaerobic conditions. Sterile wooden cotton swabs were dipped into the overnight cultures and streaked onto respective media agar plates to form a continuous lawn of bacterial growth. Stock solutions of the compound library at 100 mM in DMSO were diluted into media to a final concentration of 100 μM. A vehicle control of DMSO was diluted in the same way. Blank BDL-sensi-discs (6 mm) were incubated with the 100 μM compounds or vehicle control at room temperature for 20 min. BDL-antibiotic laden discs containing levofloxacin (5 μg), gentamicin (10 μg), and gentamicin (120 μg) were used as controls for antibiotic sensitivity. Discs were subsequently placed onto the bacterial streaked agar plates and incubated overnight at 37°. Zones of inhibition representing antibiotic and/or compound sensitivity were measured in mm for each of the antibiotics, compounds, and vehicle controls. The same assay using pathogenic bacteria *Listeria monocytogenes* 10403 (RM2194) and *Salmonella enterica* pGFP was carried out as described above.^{30,31}

X-ray structure determination

Single-crystal X-ray diffraction data were collected on a Bruker KAPPA APEX II DUO diffractometer using graphite-monochromated Mo-K α radiation ($\lambda = 0.71073$ Å). The data collection was carried out at 173(2) K. The temperature was controlled by an Oxford Cryostream cooling system (Oxford Cryostat). Cell refinement and data reduction were performed using the program SAINT.³⁵ The data were scaled and absorption correction performed using SADABS.³² The structure was solved by direct methods using SHELXS-97³⁶ and refined by full-matrix least-squares methods based on F^2 using SHELXL-2014³⁶ and using the graphics interface program X-Seed.³⁷ The programs X-Seed, POV-Ray³⁸ and Ortep³⁹ were used to prepare molecular graphic images.

Acknowledgements

Financial support from the University of Cape Town (UCT) and the National Research Foundation (NRF) of South Africa (Grant No.: 90500) and the Medical Research Council (MRC) of South Africa is gratefully acknowledged. C. T. and L. W. C. were funded by the U. S. Department of Agriculture, Agricultural Research Service (National Program 108, Project #5325-

42000-049-00D). K. M. L. was supported by the Department of Biological Sciences, the University of the Pacific.

References

- 1 The World Health Organisation, World Malaria Report 2014, http://www.who.int/malaria/media/world_malaria_report_2014/en/.
- 2 M. Enserink, *Science*, 2010, **328**, 844–846.
- 3 C. Biot, W. Castro, C. Y. Botte and M. Navarro, *Dalton Trans.*, 2012, **41**, 6335–6349.
- 4 M. Navarro, M. Castro and C. Biot, *Organometallics*, 2012, **31**, 5715–5727.
- 5 P. F. Salas, C. Herrmann and C. Orvig, *Chem. Rev.*, 2013, **113**, 3450–3492.
- 6 C. Biot, G. Glorian, L. A. Macejewski, J. S. Brocard, O. Domarle, G. Blampain, P. Millet, A. J. Georges, H. Abessolo and D. Dive, *J. Med. Chem.*, 1997, **40**, 3715–3718.
- 7 F. Dubar, T. J. Egan, B. Pradines, D. Kuter, K. K. Ncokezi, D. Forge, J. F. Paul, C. Pierrot, H. Kalamou, J. Khalife, E. Buisine, C. Rogier, H. Vezin, I. Forfar, C. Slomianny, X. Trivelli, S. Kapishnikov, L. Leiserowitz, D. Dive and C. Biot, *Chem. Biol.*, 2011, **6**, 275–287.
- 8 S. D. Khanye, J. Gut, P. J. Rosenthal, K. Chibale and G. S. Smith, *J. Organomet. Chem.*, 2011, **696**, 3296–3300.
- 9 T. Stringer, D. Taylor, C. de Kock, H. Guzgay, A. Au, S. H. An, B. Sanchez, R. O'Connor, N. Patel, K. M. Land, P. J. Smith, D. T. Hendricks, T. J. Egan and G. S. Smith, *Eur. J. Med. Chem.*, 2013, **69**, 90–98.
- 10 T. Stringer, D. Taylor, H. Guzgay, A. Shokar, A. Au, P. J. Smith, D. T. Hendricks, K. M. Land, T. J. Egan and G. S. Smith, *Dalton Trans.*, 2015, **44**, 14906–14917.
- 11 D. Soper, *Am. J. Obstet. Gynecol.*, 2004, **190**, 281–290.
- 12 D. F. Harp and I. Chowdhury, *Eur. J. Obstet. Gynecol. Reprod. Biol.*, 2011, **157**, 3–9.
- 13 C. C. Musonda, S. Little, V. Yardley and K. Chibale, *Bioorg. Med. Chem. Lett.*, 2007, **17**, 4733–4736.
- 14 D. P. Iwaniuk, E. D. Whetmore, N. Rosa, K. Ekoue-Kovi, J. Alumasa, A. C. De Dios, P. D. Roepe and C. Wolf, *Bioorg. Med. Chem.*, 2009, **17**, 6560–6566.
- 15 M. R. Valderrama, R. V. García, T. Klimova, E. Klimova, L. Ortiz-Frade and M. M. García, *Inorg. Chim. Acta*, 2008, **361**, 1597–1605.
- 16 N. Baartzes, T. Stringer, R. Seldon, D. F. Warner, C. de Kock, P. J. Smith and G. S. Smith, *J. Organomet. Chem.*, 2016, **809**, 79–85.
- 17 P. F. Salas, C. Herrmann, J. F. Cawthray, C. Nimphius, A. Kenkel, J. Chen, C. de Kock, P. J. Smith, B. O. Patrick, M. J. Adam and C. Orvig, *J. Med. Chem.*, 2013, **56**, 1596–1613.
- 18 C. Biot, W. Daher, C. M. Ndiaye, P. Melnyk, B. Pradines, N. Chavain, A. Pellet, L. Fraisse, L. Pelinski, C. Jarry, J. Brocard, J. Khalife, I. Forfar-Bares and D. Dive, *J. Med. Chem.*, 2006, **49**, 4707–4714.



- 19 D. Dive and C. Biot, *ChemMedChem*, 2008, **3**, 383–391.
- 20 N. Sunduru, K. Srivastava, S. Rajakumar, S. K. Puri, J. K. Saxena and P. M. S. Chauhan, *Bioorg. Med. Chem. Lett.*, 2009, **19**, 2570–2573.
- 21 R. Buller, M. L. Peterson, O. Almarrson and L. Leiserowitz, *Cryst. Growth Des.*, 2002, **2**, 553–562.
- 22 R. D. Sandlin, M. D. Carter, P. J. Lee, J. M. Auschwitz, S. E. Leed, J. D. Johnson and D. W. Wright, *Antimicrob. Agents Chemother.*, 2011, **55**, 3363–3369.
- 23 A. N. Hoang, K. K. Ncokazi, K. A. De Villiers, D. W. Wright and T. J. Egan, *Dalton Trans.*, 2010, **39**, 1235–1244.
- 24 A. N. Hoang, R. D. Sandlin, A. Omar, T. J. Egan and D. W. Wright, *Biochemistry*, 2010, **49**, 10107–10116.
- 25 K. K. Ncokazi and T. J. Egan, *Anal. Biochem.*, 2005, **338**, 306–319.
- 26 P. Govender, A. K. Renfrew, C. M. Clavel, P. J. Dyson, B. Therrien and G. S. Smith, *Dalton Trans.*, 2011, **40**, 1158–1167.
- 27 P. Govender, T. Riedel, P. J. Dyson and G. S. Smith, *J. Organomet. Chem.*, 2015, **799**, 38–44.
- 28 J. Rajput, J. R. Moss, A. T. Hutton, D. T. Hendricks, C. E. Arendse and C. Imrie, *J. Organomet. Chem.*, 2004, **689**, 1553–1568.
- 29 A. R. Martirosyan, R. Rahim-Bata, A. B. Freeman, C. D. Clarke, R. L. Howard and J. S. Strobl, *Biochem. Pharmacol.*, 2004, **68**, 1729–1738.
- 30 A. Bauer, W. M. M. Kirby, J. C. Sherris and M. Turck, *Am. J. Clin. Pathol.*, 1966, **36**, 493–496.
- 31 J. H. Jorgensen and J. D. Turnidge, Susceptibility test methods: dilution and disk diffusion methods, in *Manual of clinical microbiology*, ed. P. R. Murray, E. J. Baron, J. H. Jorgensen, M. L. Landry and M. A. Pfaller, ASM Press, Washington D.C., 9th edn, 2007, pp. 1152–1172.
- 32 W. Trager and J. B. Jensen, *Science*, 1976, **193**, 673–675.
- 33 M. T. Makler, J. M. Ries, J. A. Williams, J. E. Bancroft, R. C. Piper, B. L. Gibbins and D. J. Hinrichs, *Am. J. Trop. Med. Hyg.*, 1993, **48**, 739–741.
- 34 J. Van Meerloo, G. J. L. Kaspers and J. Cloos, in *Cancer Cell Culture: Methods and Protocols (Methods in Molecular Biology)*, ed. I. A. Cree, Humana Press, 2011, pp. 237–245.
- 35 *SAINT Version 7.60a*, Bruker AXS Inc., Madison, WI, USA, 2006.
- 36 G. M. Sheldrick, *SHELXS-97, SHELXL-2014 and SADABS version 2.05*, University of Göttingen, Germany, 1997.
- 37 (a) L. J. Barbour, *J. Supramol. Chem.*, 2001, **1**, 189–191; (b) J. L. Atwood and L. J. Barbour, *Cryst. Growth Des.*, 2003, **3**, 3.
- 38 Persistence of Vision Raytracer, <http://www.povray.org/>.
- 39 L. J. Farrugia, *J. Appl. Crystallogr.*, 2012, **45**, 849–854.

